

Intranight variability of ultraviolet emission from high- z blazars

Krishan CHAND

Aryabhata Research Institute of Observational Sciences (ARIES), Manora Peak, Nainital –
263002, India

Correspondance to: krishanchand007.kc@gmail.com

Abstract

Rapid intranight variability of continuum and polarization in blazars is a very useful tool to probe the beaming of a relativistic jet and the associated population of the relativistic particles. Such intranight variability in the rest-frame optical continuum has been carried out extensively, but there is a scarcity of such information in the rest-frame ultra-violet (UV), where the cause of variability might be due to a secondary population of relativistic particles. To fill this gap, recently in Chand et al. (2022) we reported for the first time intranight variability study of a sample of high- z blazars so that the monitored optical radiation is their rest-frame UV radiation. Here we discuss in detail the implication of this investigation with a proper comparison of high- z blazar samples with fractional optical polarization (p_{opt}) smaller and higher than 3%. In this context, we also report intranight variability study of an additional high- z blazar at $z=2.347$, namely J161942.38+525613.41, monitored over three sessions each with a duration of ~ 5 hr. Our investigation does not reveal any compelling evidence for a stronger intranight variability of UV emission for high polarization blazars, in contrast to the blazars monitored in the rest-frame blue-optical. We also discuss this trend in light of the proposal that the synchrotron radiation of blazar jets in the UV/X-ray regime may arise from a relativistic particle population different from that radiating up to near-infrared/optical frequencies.

Keywords: galaxies: active – galaxies: photometry – galaxies: high-redshift – galaxies

1. Introduction

Blazars are radio-loud active galactic nuclei (AGN) whose radiation is mostly non-thermal. The origin of radiation is a relativistic jet that is roughly directed and hence beamed towards the observer (Blandford and Rees, 1978; Moore and Stockman, 1984; Urry and Padovani, 1995). The radiation appears highly Doppler boosted in our direction due to beaming and hence completely dominates the radiation coming from the host galaxy and accretion disk. Rapid variability of continuum and polarized emission, and a flat radio spectrum (i.e., a dominant radio core) are well-known characteristics of beaming. The quasar subset of blazars with a higher power is known as flat-spectrum radio quasars (FSRQs) (e.g., Stockman et al., 1984; Wills et al., 1992; Angelakis et al., 2016). Their jets frequently show superluminal motion as well as large variability amplitude at all wavelengths from radio to γ -rays. The flux variability from radio to

optical, and even TeV bands has been very useful for unveiling the physics of blazars, particularly the extreme cases of flux variability observed on hour-like or even shorter time-scales (e.g., Wagner and Witzel, 1995; Aharonian et al., 2017; Gopal-Krishna and Wiita, 2018).

The UV band is one important spectral region for which little information about intranight variability is available. The primary reason for the lack of information about the rapid UV variability of AGN is that intranight monitoring campaigns for space-borne UV telescopes are prohibitively time expensive. Although, in recent years, there have been attempts to fill this information gap by using UV data acquired with GALEX for large AGN samples; however, such studies have covered only day-like or longer time-scales and are particularly devoted to optically selected quasars (e.g., Punsly et al., 2016; Xin et al., 2020). Hence, these studies may well have had substantial contributions from the accretion disk and not have measured only UV emission of synchrotron origin. Additionally, from detailed measurements of spectral energy distribution (SED) of a few quasar jets, a hint regarding UV radiation has emerged, according to which a very substantial, if not dominant contribution to synchrotron UV radiation of quasar jets may arise from a relativistic particle population distinct from the one responsible for their radiation up to near-infrared and optical frequencies. Specifically, the SED of the knots in the kiloparsec-scale radio jets of some quasars is found to exhibit a sharp spectral *upturn* towards the UV and connecting smoothly thereafter to the X-ray data points (Uchiyama et al., 2006, 2007; Jester et al., 2007). Moreover, the observed high polarization in the UV emission supports a synchrotron interpretation for this higher-energy radiation component (Cara et al., 2013). The above-mentioned studies support the idea that the optical and UV radiations from jets are synchrotron radiation arising from two different populations of relativistic particles. This idea was recently reinforced by Chand et al. (2022) by comparing the intranight flux variability of blazars at rest-frame UV and optical wavelengths.

In order to probe the rapid UV variability of blazars, the practical approach adopted by Chand et al. (2022) is that they carried out *optical* intranight monitoring of 14 blazars (FSRQs), located at very high redshifts ($1.5 < z < 3.7$), so that their monitored optical radiation is actually UV emission in the rest-frame. Their study consisted of two prominent subclasses of blazars, distinguished by low and high fractional polarization measured in the optical, with division taken at $p_{opt} = 3\%$ (Moore and Stockman, 1984). This resulted in (i) nine low-polarization FSRQs with $p_{opt} < 3\%$ and five high-polarization FSRQs with $p_{opt} > 3\%$. Based on the photometric statistical analysis for nine low-polarization FSRQs and five high-polarization FSRQs, they found no evidence for a strong correlation of intranight variability of UV emission with polarization, in contrast to the strong correlation found for intranight variability of optical emission. This led them to a proposal that the synchrotron radiation of blazar jets in the UV/X-ray regime arises from a relativistic particle population distinct from the one responsible for their synchrotron radiation up to near-infrared/optical frequencies. Since their two samples are too small to be representative of the high- z blazar population, this finding might be spurious. Hence, an independent check on this finding is required which can be achieved through intranight optical monitoring of a larger sample of high- z blazars with low and high polarization. To make the above finding statistically more robust, we made an enlarged sample of 34 high- z blazars which is 2.4 times larger than the combined sample of low-polarization and high-polarization blazars

reported in Chand et al. (2022) (see section 2). The major obstacle in enlarging the sample of high- z blazars for studying intranight variability of rest-frame UV emission with polarization is the lack of polarization information in the literature. And it is essential to have high- z blazars with low and high polarization to explore the dependence of intranight UV variability with polarization. More than half of the sources (19) in an enlarged sample of 34 high- z blazars also lack polarization information in the literature; therefore, the purpose of the intranight variability study of UV emission for an enlarged sample of high- z blazars is two-folded: (i) polarization measurements of the sources and (ii) intranight optical monitoring of the sources. The selected 34 high- z blazars have a brightness (m_R) range from 15.2 to 17.4 and to detect the polarization of a few per cent within this brightness range requires telescopes of at least 2-3 metres in diameter. Therefore, for polarization measurements, we are making proposals in consideration of the impending availability of an imaging polarimeter at the 3.6-m Devasthal Optical Telescope (DOT) at ARIES and the intranight optical monitoring will be carried out using metre-class telescopes available in India.

The polarization and intranight optical observations for high- z blazar samples in Chand et al. (2022) are separated by a median time of four years. The fluctuation in the polarization state of around a quarter of FSRQs on a year-like time-scale has been reported in various studies (Impey and Tapia, 1990; Chand and Gopal-Krishna, 2022; Chand et al., 2023). Owing to the variable nature of polarization for blazars, the two sets of observations i.e., polarimetric and photometric observations should be quasi-simultaneous. However, it is quite challenging to conduct both polarimetric and photometric observations simultaneously. It should be noted that there exists a strong correlation between intranight optical variability (INOV) and p_{opt} for moderately distant blazars despite the fact that the two sets of observations were made a decade apart (Goyal et al., 2012, and references therein). It is also known that the long-term optical variability is stronger for sources with large p_{opt} (e.g., Angelakis et al., 2016). It will be useful not only to enlarge the sample of high- z blazars for studying the intranight variability of the UV continuum but also to conduct intranight photometric observations in conjunction with their quasi-simultaneous polarimetric observations. This forms the main motivation of this article, where we devise a large sample of 34 high- z blazars for intranight variability and quasi-simultaneous polarimetric observations based on the upcoming imaging polarimeter at 3.6-m DOT. In this ongoing long-term project, we present the intranight optical monitoring of one of the 34 high- z blazars, namely J161942.38+525613.41 at $z = 2.347$, in three sessions with a median duration of ~ 5 hr.

The article is organised as follows. In section 2, we present a selection of enlarged sample along with notes on the J161942.38+525613.41. Section 3 details about photometric monitoring and data reduction, while statistical analysis is briefly given in section 4. Finally, we present our detailed discussion and conclusion in section 5.

2. The enlarged sample of high- z blazars

The enlarged sample of high- z blazars for intranight optical and polarimetric monitoring was derived from the 3561 sources listed in the 5th edition of the ROMA blazar catalogue

(ROMA-BZCAT, Massaro et al., 2015). These sources are either confirmed blazars or exhibit blazar-like characteristics. The redshift requirement of $z > 1.5$ was first applied to 3651 sources, and 784 blazars were found to meet this criterion. Then, we applied a brightness filter i.e., $m_R < 17.5$ to 784 blazars, to ensure a good SNR with metre-class telescopes. This resulted in 84 blazars, of which 41 were discarded due to their negative declinations. Nine additional sources were also omitted because a long intranight monitoring session was not possible as these sources transit at night during the monsoon period. Thus, the final enlarged sample of high- z blazars consists of 34 sources with redshift $z > 1.5$. Of the 34 blazars, nine sources were already reported in Chand et al. (2022). In this article, we have provided the INOV results for one of the 34 high- z blazars, namely, J161942.38+525613.41 along with the previously reported results for blazars in Chand et al. (2022) and the notes on this source are given below:

J161942.38+525613.41: It is an FSRQ type of blazar with a brightness (m_R) of 16.7 mag (Massaro et al., 2015). It is located at a redshift of 2.347 (Peña-Herazo et al., 2021) with the logarithmic bolometric luminosity of 47.78 erg s^{-1} (Rakshit et al., 2020), making it a member of the high-luminosity tail of blazars. The source has detection in radio bands having a flux density of 182 mJy and 128 mJy at 1.4 GHz (Condon et al., 1998) and 5 GHz (Gregory et al., 1996) respectively. A flat radio spectral index (α_r) of -0.07 (Bourda et al., 2010), signifies the core dominance of the source. Due to its high- z of 2.347, the monitored optical radiation is actually rest-frame UV emission and Rakshit et al. (2020) estimated a logarithmic continuum luminosity of 47.19 erg s^{-1} and 46.84 erg s^{-1} at 1350 \AA and 3000 \AA respectively.

3. Photometric Monitoring and Data Reduction

We carried out the intranight photometric observations of the high- z FSRQ J161942.38+525613.41 ($z=2.347$) in Johnson-Cousins R or SDSS r-band in three sessions with a median duration of 5.06 hr. The 1.04-m Sampuranand Telescope (ST; Sagar 1999, two sessions) and the 3.6-m Devasthal Optical Telescope (DOT; Kumar et al. 2018, one session) are the telescopes that were employed. The observations for the ST sessions were taken with $4k \times 4k$ CCD fixed at the focal plane of ST which is of Ritchey Chretien (RC) type (Sagar, 1999). The $4k \times 4k$ CCD were cooled to -120°C using liquid nitrogen to minimise the dark noise. The CCD has a pixel size of 15 microns and a plate scale of 0.23 arcsec per pixel, thus covering a field of view (FOV) of $15 \times 15 \text{ arcmin}^2$ on the sky. The observations were conducted in 4×4 binning mode at a gain of $3e^-$ per ADU and a readout speed of 1 MHz with a readout noise of $7e^-$. For the DOT session, the observations were acquired with the ARIES Devasthal-Faint Object Spectrograph and Camera (ADFOSC) mounted at the Cassegrain main port of the DOT which is also of Ritchey Chretien (RC) design (Kumar et al., 2018). ADFOSC is equipped with a deep depletion $4k \times 4k$ CCD, cooled to -120°C using a closed-cycle cryo cooling thermal engine having a pixel size of 15 microns, a plate scale of ~ 0.2 arcsec per pixel, hence covering a $13.6 \times 13.6 \text{ arcmin}^2$ FOV on the sky (Omar et al., 2019). The observations were also carried out in 4×4 binning mode with a readout noise of $8e^-$ at a speed of ~ 0.2 MHz and a gain of $1e^-$ per ADU.

The pre-processing of the raw images (bias subtraction, flat-fielding and cosmic ray removal) was done using the standard tasks available in the Image Reduction and Analysis Fa-

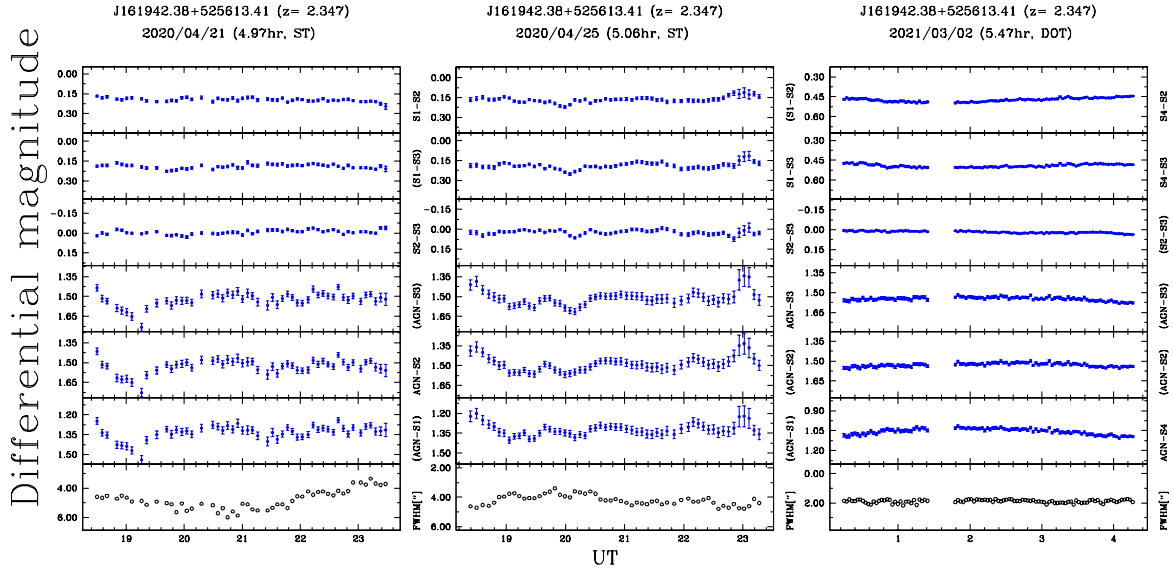


Figure 1: Differential light curves (DLCs) for the high- z FSRQ, J161942.38+525613.41. The date and duration of the observation along with the name of the source J161942.38+525613.41 are given at the top of each night’s data. The upper three panels give the comparison star-star DLCs, whereas the subsequent lower panels give the source-star DLCs as described by the labels on the right side. The bottom panel gives the variation in seeing during the course of observation.

cility (IRAF). The instrumental magnitudes of the target source and the selected three comparison stars in the CCD frames were determined through aperture photometry (Stetson, 1987, 1992), using the Dominion Astronomical Observatory Photometry II (DAOPHOT II) algorithm. The aperture radius, a very crucial parameter for photometry was determined by averaging the FWHM of the point spread function (PSF) of five moderately bright stars. In the present case, we fixed the aperture radius equal to $2 \times \text{PSF}$ since the SNR was found to be the highest for this aperture (see Chand et al., 2022). We then derived differential light curves (DLCs) for the target source relative to the three selected comparison stars in the same CCD frames which are within 1.5 magnitudes of the target source (see Table 1).

Table 1: Basic parameters of selected comparison stars for high- z J161942.38+525613.41.

Object	Date	R.A.(J2000)	Dec.(J2000)	g	r	$g-r$
(1)	yyyy/mm/dd	(hh:mm:ss)	($^{\circ}$: $'$: $''$)	(mag)	(mag)	(mag)
	(2)	(3)	(4)	(5)	(6)	(7)
J161942.38+525613.41	2020/04/21, 2020/04/25, 2021/03/02	16:19:42.38	+52:56:13.41	16.82	16.74	0.08
S1	2020/04/21*, 2020/04/25*	16:19:32.72	+52:49:35.19	16.41	15.53	0.88
S2	2020/04/21, 2020/04/25*, 2021/03/02*	16:19:48.69	+52:58:19.60	16.05	15.37	0.68
S3	2020/04/21*, 2020/04/25, 2021/03/02*	16:19:37.29	+52:58:44.68	15.92	15.33	0.59
S4	2021/03/02	16:20:14.60	+52:52:17.80	16.36	15.88	0.48

The comparison stars on a particular marked session (*) have been used to determine the INOV status of AGN.

4. Statistical Analysis

In the current analysis, we have employed the F_η test to determine whether INOV exists in the derived DLCs or not (Chand et al., 2022; Gopal-Krishna et al., 2023). We further identified the two most stable comparison stars out of the three that were initially selected for a given session and applied the F_η test to the three DLCs involving only them (the selected two comparison stars for each session are shown within parentheses in column 5 of Table 2 and the corresponding DLCs are also labelled within parentheses in Fig. 1 on the right side). In several independent studies, it has been found that the photometric errors returned by DAOPHOT are too small (Gopal-Krishna et al., 1995; Garcia et al., 1999; Sagar et al., 2004; Stalin et al., 2004; Bachev et al., 2005; Goyal et al., 2012, 2013a) and the best value for the underestimation factor η is found to be 1.54 ± 0.05 , based on 262 monitoring sessions of quasars/blazars (Goyal et al., 2013b) and the same value has been used in this study. The F-values for the selected two blazar DLCs in a given session are:

$$F_1^\eta = \frac{\text{Var}(q - s1)}{\eta^2 \sum_{i=1}^N \sigma_{i,err}^2(q - s1)/N}, \quad F_2^\eta = \frac{\text{Var}(q - s2)}{\eta^2 \sum_{i=1}^N \sigma_{i,err}^2(q - s2)/N} \quad (1)$$

where $\text{Var}(q - s1)$ and $\text{Var}(q - s2)$ are the variances of the target source relative to star1 and star2 respectively. And $\sigma_{i,err}^2(q - s1)$ and $\sigma_{i,err}^2(q - s2)$ denote the errors that DAOPHOT returned for each individual data point of the target source relative to star1 and star2 respectively. N is the total number of data points taken in observation (Column 3 of Table 2) and $\eta = 1.54$ is the scaling factor, as mentioned above. The computed value of F_1^η and F_2^η for the target source–star DLCs are given in Table 2, column 5.

The F–values estimated from the $F_{1,2}^\eta$ test (Column 5 from Table 2) are compared with the critical value of F (F_c^α) for $\alpha = 0.05, 0.01$ corresponding to confidence levels of 95% and 99%, respectively (Column 6,7 in Table 2). If the computed F–value exceeds the critical value, the null hypothesis (i.e., no variability) is discarded. We thus classify a source with F–value $\geq F_c(0.99)$ as a variable (‘V’) at confidence level ≥ 0.99 ; probably variable (‘PV’) for F–value between $F_c(0.95)$ and $F_c(0.99)$, and non-variable (‘NV’) if the computed F–value is less than $F_c(0.95)$. In the F_η test where two F–values involved are related to comparison stars 1 and 2, we set the class of a target source as variable (‘V’) if F–value calculated for both source–star1 and source–star2 DLCs exceeds the value $F_c(0.99)$. And the target source is considered as a non-variable (‘NV’) if F–value for at least one of the source–star DLCs is less than the $F_c(0.95)$. For other remaining situations i.e., a combination of V, PV or PV, PV, the target source is classified as a probable variable (‘PV’). Column 10 in Table 2 lists the ‘Photometric Noise Parameter’ (PNP) = $\sqrt{\eta^2 \langle \sigma_{i,err}^2 \rangle}$, estimated for a monitoring session using the star–star DLCs, where $\eta = 1.54$, as mentioned above.

To make the variability results more convincing, we attempted to derive the DLCs using the same set of three comparison stars (S1, S2 & S3) for the two ST and one DOT sessions observed on April 21, 2020, April 25, 2020, and March 02, 2021, respectively. However, due to the lack of steadiness of S1 for the DOT session observed on March 02, 2021, a new stable comparison star S4 was used instead of S1. Since the F_η test incorporates two comparison stars,

Table 2: Result of the statistical test for detecting INOV in the DLCs of the J161942.38+525613.41.

Blazar (SDSS name) (1)	Date yyyy/mm/dd (2)	N (3)	T (hr) (4)	F_1^η, F_2^η (5)	F-test $F_c(0.95)$ $F_c(0.99)$ (6) (7)		INOV status ^a (8) (9)		$\sqrt{\eta^2 \langle \sigma_{i, err}^2 \rangle}$ (10)	$\bar{\psi}$ % (11)
J161942.38+525613.41	21/04/2020	51	4.97	1.83 (S1), 1.78 (S3)	1.60	1.95	PV, PV	PV	0.015 (S1-S3)	29.60
J161942.38+525613.41	25/04/2020	58	5.06	0.60 (S1), 0.62 (S2)	1.55	1.87	NV, NV	NV	0.037 (S1-S2)	—
J161942.38+525613.41	02/03/2021	138	5.47	6.63 (S2), 9.62 (S3)	1.33	1.49	V, V	V	0.005 (S2-S3)	15.89

^a V=variable, i.e., confidence ≥ 0.99 ; PV = probable variable (0.95 – 0.99); NV = non-variable (< 0.95).

Variability status identifiers (col. 8), based on AGN-star1 and AGN-star2 DLCs are separated by a comma.

we further identified the two most stable comparison stars out of the three for the observed sessions as mentioned above. We found a set of stable comparison stars (S1, S2 & S3) in different combinations for the two ST and one DOT sessions (see Table 2, also, Fig. 1). If we look at Fig. 1, it is easy to believe that there are significant variations on the first night and a good chance that there are some on the second night, but there is little chance of real variability on the third night, except perhaps for a slow rise and fall. However, based on the F_η test, Table 2 indicates that the first is PV, the second is NV, and the last is V. Presumably, this non-obvious result comes from some combination of the larger number of data points that could be measured in the same amount of time at the larger DOT than at ST as well as the smaller error bars at DOT.

The INOV variability amplitude (ψ , see Table 2, column 11) was computed using the definition given by (Heidt and Wagner, 1996):

$$\psi = \sqrt{(A_{max} - A_{min})^2 - 2\sigma^2}$$

Here A_{max} and A_{min} are the maximum and minimum values in the source-star DLC and $\sigma^2 = \eta^2 \langle \sigma_{q-s}^2 \rangle$, where, σ_{q-s}^2 is the mean square rms error for the data points in the DLC and $\eta = 1.54$. The mean value of ψ for a session, i.e., the average of the ψ values estimated for the two selected DLCs of the target source is given in column 11 of Table 2.

5. Discussion and Conclusion

The R-band/r-band intranight monitoring reported in Chand et al. (2022) for the two samples of high- z blazars corresponds to their rest-frame UV emission. For sources in their first sample (nine LP_{FSRQs}), the rest-frame wavelengths of monitoring are from 1374 Å to 2078 Å (median 1973 Å), while for their second sample (five HP_{FSRQs}), the corresponding range is from 2078 Å to 2495 Å (median 2099 Å). The rest-frame wavelength of the high- z FSRQ J161942.38+525613.41, located at a redshift of 2.347 is 1914 Å, thus making it a suitable source for studying the intranight variability of UV emission.

Chand et al. (2022) estimated the duty cycle (DC) of $\sim 30\%$ with $\psi > 3\%$ for the intranight variability of nine LP_{FSRQs} at median $z \sim 2.25$. For five HP_{FSRQs} at median $z \sim 2.0$, the DC of intranight variability was estimated to be $\sim 12\%$ with $\psi > 3\%$. On two counts, the results of F_η test for nine LP_{FSRQs} and five HP_{FSRQs} are different from the past INOV estimates using the same F_η test. Firstly, Goyal et al. (2013a) estimated an INOV DC of $\sim 10\%$ for $\psi > 3\%$ cases, using a large sample of 12 moderately distant (median $z \sim 0.7$) LP_{FSRQs} monitored in

43 intranight sessions of > 4 hr duration. In the same study, the INOV DC was found to be $\sim 38\%$ for $\psi > 3\%$, for a sample of 11 moderately distant (median $z \sim 0.7$) HP_{FSRQs} monitored in 31 sessions. It should be noted that based on these results, a strong correlation between intranight optical variability (INOV) and p_{opt} was established for moderately distant blazars despite the fact that the two sets of observations were made a decade apart. This indicates that the propensity of a given FSRQ to exhibit strong INOV is of a fairly stable nature and it correlates tightly with the optical polarization class.

The DC of $\sim 30\%$ for high- z LP_{FSRQs} is considerably higher than that of their lower- z counterparts (DC $\sim 10\%$) and is quite comparable to their lower- z HP_{FSRQs} . The excess of DC found for high- z LP_{FSRQs} (DC $\sim 30\%$) could possibly be even greater given that their sample of LP_{FSRQs} is heavily biased towards the most luminous members of this AGN class and variability is known to anti-correlate with luminosity from several studies (e.g., Guo and Gu, 2014). However, it is still unknown whether the anti-correlation with luminosity is significant on the intranight time scales since so far, it has been established only for variability on month/year-like time scales. One possible explanation offered by Chand et al. (2022) for the high DC of LP_{FSRQs} is that some of their members are actually HP_{FSRQs} but were mistakenly categorised as LP_{FSRQs} since their observed polarization, p_{opt} (i.e., rest-frame UV polarization) has been decreased due to dilution by thermal UV from the accretion disc.

Secondly, their second sample of five HP_{FSRQs} did not support the above explanation. They estimated an INOV DC of $\sim 12\%$ for five HP_{FSRQs} which is quite low, and these HP_{FSRQs} can not be misidentified as LP_{FSRQs} since thermal dilution only lowers the polarization. Furthermore, Chand et al. (2022) looked for the observational biases (i.e., the intrinsic duration of monitoring and photometric sensitivity) that could have spuriously led to higher DC for LP_{FSRQs} in comparison to HP_{FSRQs} . They found that the intrinsic duration of monitoring and photometric sensitivity for LP_{FSRQs} and HP_{FSRQs} is very similar. Hence, the possibility of observational biases was discarded. In summary, based on the results for nine LP_{FSRQs} and five HP_{FSRQs} , a strong correlation of intranight variability of UV emission with polarization could not be found, in contrast to the strong correlation found for intranight variability of optical emission.

To this astonishing result, we now added three intranight sessions of FSRQ J161942.38+525613.41 located at $z = 2.347$, monitored in R-band/r-band with a median duration of ~ 5 hr using ST and DOT. Since the polarization information is unavailable in the literature, the FSRQ J161942.38+525613.41 could not be classified as LP_{FSRQ} or HP_{FSRQ} . Therefore, the FSRQ J161942.38+525613.41 was included in both the samples of Chand et al. (2022) while estimating the INOV DC. For estimating the INOV DC, only the type ‘V’ sessions with confirmed variability of $\psi > 3\%$ were used. Only one session was found to be variable (‘V’) with $\psi > 3\%$, observed on March 02, 2021 using DOT (see, Column 9 of Table 2). A high DC of $\sim 30\%$ with an amplitude of $\psi > 3\%$ was estimated for intranight variability of low-polarization FSRQs even after including the FSRQ J161942.38+525613.41 as a low-polarization FSRQ. Similarly, when the source J161942.38+525613.41 was taken into account as a high-polarization FSRQ, the estimated DC was found to be $\sim 16\%$ with an amplitude of $\psi > 3\%$ which is still fairly low. Thus, we found no evidence for a strong intranight variability of UV emission with polariza-

tion even after including the FSRQ J161942.38+525613.41 as a low/high-polarization FSRQ, in contrast to the blazars monitored in the rest-frame blue-optical. This supports the proposal put forth in Chand et al. (2022) that the synchrotron radiation of blazar jets in the UV/X-ray regime arises from a relativistic particle population distinct from the one responsible for their synchrotron radiation up to near-infrared/optical frequencies. However, the measurement of polarization for the FSRQ J161942.38+525613.41 using the upcoming imaging polarimeter at 3.6-m DOT will make the source either LP_{FSRQs} or HP_{FSRQs} , resulting in an increment of the size of one of two blazar samples of Chand et al. (2022) by just one which is again small. The two blazar samples are yet too small to be representative of the high- z blazar population, so the above finding might be spurious. Hence, this interesting finding requires independent confirmation through intranight optical monitoring of a larger sample of high- z blazars with low and high polarization. Consequently, an enlarged sample of 34 high- z blazars was derived from the ROMA-BZCAT catalogue to verify the above finding which we intend to observe in future using metre-class telescopes available in India (see section 1, also, section 2).

Acknowledgments

We thank Prof. Paul J. Wiita for his valuable comments and suggestions for improving the quality of the manuscript. We thank the organisers for allowing us to present our work at the BINA conference and for the local support. We also thank Prof. Hum Chand for his thoughtful suggestions and discussion regarding the current work.

Further Information

ORCID identifiers of the authors

0000-0002-6789-1624 (Krishan CHAND)

Conflicts of interest

The author declares no conflict of interest.

References

- Aharonian, F. A., Barkov, M. V. and Khangulyan, D. (2017) Scenarios for Ultrafast Gamma-Ray Variability in AGN. *ApJ*, 841(1), 61. <https://doi.org/10.3847/1538-4357/aa7049>.
- Angelakis, E., Hovatta, T., Blinov, D., Pavlidou, V., Kiehlmann, S., Myserlis, I., Böttcher, M., Mao, P., Panopoulou, G. V., Liodakis, I., King, O. G., Baloković, M., Kus, A., Ky-lafis, N., Mahabal, A., Marecki, A., Paleologou, E., Papadakis, I., Papamastorakis, I., Pazderski, E., Pearson, T. J., Prabhudesai, S., Ramaprakash, A. N., Readhead, A. C. S.,

- Reig, P., Tassis, K., Urry, M. and Zensus, J. A. (2016) RoboPol: the optical polarization of gamma-ray-loud and gamma-ray-quiet blazars. *MNRAS*, 463(3), 3365–3380. <https://doi.org/10.1093/mnras/stw2217>.
- Bachev, R., Strigachev, A. and Semkov, E. (2005) Short-term optical variability of high-redshift quasi-stellar objects. *MNRAS*, 358, 774–780. <https://doi.org/10.1111/j.1365-2966.2005.08708.x>.
- Blandford, R. D. and Rees, M. J. (1978) Extended and compact extragalactic radio sources: interpretation and theory. *PhysS*, 17, 265–274. <https://doi.org/10.1088/0031-8949/17/3/020>.
- Bourda, G., Charlot, P., Porcas, R. W. and Garrington, S. T. (2010) VLBI observations of optically-bright extragalactic radio sources for the alignment of the radio frame with the future Gaia frame. I. Source detection. *A&A*, 520, A113. <https://doi.org/10.1051/0004-6361/201014248>.
- Cara, M., Perlman, E. S., Uchiyama, Y., Cheung, C. C., Coppi, P. S., Georganopoulos, M., Worrall, D. M., Birkinshaw, M., Sparks, W. B., Marshall, H. L., Stawarz, L., Begelman, M. C., O’Dea, C. P. and Baum, S. A. (2013) Polarimetry and the High-energy Emission Mechanisms in Quasar Jets: The Case of PKS 1136-135. *ApJ*, 773(2), 186. <https://doi.org/10.1088/0004-637X/773/2/186>.
- Chand, K. and Gopal-Krishna (2022) Persistence of the blazar state in flat-spectrum radio quasars. *MNRAS*, 516(1), L18–L23. <https://doi.org/10.1093/mnrasl/slac066>.
- Chand, K., Gopal-Krishna, Omar, A., Chand, H., Mishra, S., Bisht, P. S. and Britzen, S. (2022) Intranight variability of ultraviolet emission from powerful blazars. *MNRAS*, 511(1), 13–18. <https://doi.org/10.1093/mnrasl/slac129>.
- Chand, K., Gopal-Krishna, A., Omar, Chand, H. and Bisht, P. S. (2023) The transience and persistence of high optical polarisation state in beamed radio quasars. *PASA*, 40, e006. <https://doi.org/10.1017/pasa.2023.3>.
- Condon, J. J., Cotton, W. D., Greisen, E. W., Yin, Q. F., Perley, R. A., Taylor, G. B. and Broderick, J. J. (1998) The NRAO VLA Sky Survey. *AJ*, 115(5), 1693–1716. <https://doi.org/10.1086/300337>.
- Garcia, A., Sodr e, L., Jablonski, F. J. and Terlevich, R. J. (1999) Optical monitoring of quasars - I. Variability. *MNRAS*, 309, 803–816. <https://doi.org/10.1046/j.1365-8711.1999.02884.x>.
- Gopal-Krishna, Chand, K., Chand, H., Negi, V., Mishra, S., Britzen, S. and Bisht, P. S. (2023) Intranight optical variability of low-mass active galactic nuclei: a pointer to blazar-like activity. *MNRAS*, 518(1), L13–L18. <https://doi.org/10.1093/mnrasl/slac125>.
- Gopal-Krishna, Sagar, R. and Wiita, P. J. (1995) Intranight optical variability in optically selected QSOs. *MNRAS*, 274, 701–710. <https://doi.org/10.1093/mnras/274.3.701>.

- Gopal-Krishna and Wiita, P. J. (2018) Optical monitoring of Active Galactic Nuclei from ARIES. *BSRSL*, 87, 281–290.
- Goyal, A., Gopal-Krishna, Wiita, P. J., Anupama, G. C., Sahu, D. K., Sagar, R. and Joshi, S. (2012) Intra-night optical variability of core dominated radio quasars: the role of optical polarization. *A&A*, 544, A37. <https://doi.org/10.1051/0004-6361/201218888>.
- Goyal, A., Gopal-Krishna, Wiita, P. J., Stalin, C. S. and Sagar, R. (2013a) Improved characterization of intranight optical variability of prominent AGN classes. *MNRAS*, 435, 1300–1312. <https://doi.org/10.1093/mnras/stt1373>.
- Goyal, A., Mhaskey, M., Gopal-Krishna, Wiita, P. J., Stalin, C. S. and Sagar, R. (2013b) On the Photometric Error Calibration for the Differential Light Curves of Point-like Active Galactic Nuclei. *JApA*, 34(3), 273–296. <https://doi.org/10.1007/s12036-013-9183-7>.
- Gregory, P. C., Scott, W. K., Douglas, K. and Condon, J. J. (1996) The GB6 Catalog of Radio Sources. *ApJS*, 103, 427. <https://doi.org/10.1086/192282>.
- Guo, H. and Gu, M. (2014) The Optical Variability of SDSS Quasars from Multi-epoch Spectroscopy. I. Results from 60 Quasars with \geq Six-epoch Spectra. *ApJ*, 792(1), 33. <https://doi.org/10.1088/0004-637X/792/1/33>.
- Heidt, J. and Wagner, S. J. (1996) Statistics of optical intraday variability in a complete sample of radio-selected BL Lacertae objects. *A&A*, 305, 42.
- Impey, C. D. and Tapia, S. (1990) The Optical Polarization Properties of Quasars. *ApJ*, 354, 124. <https://doi.org/10.1086/168672>.
- Jester, S., Meisenheimer, K., Martel, A. R., Perlman, E. S. and Sparks, W. B. (2007) Hubble Space Telescope far-ultraviolet imaging of the jet in 3C273: a common emission component from optical to X-rays. *MNRAS*, 380(2), 828–834. <https://doi.org/10.1111/j.1365-2966.2007.12120.x>.
- Kumar, B., Omar, A., Maheswar, G., Pandey, A. K., Sagar, R., Uddin, W., Sanwal, B. B., Bangia, T., Kumar, T. S., Yadav, S., Sahu, S., Pant, J., Reddy, B. K., Gupta, A. C., Chand, H., Pandey, J. C., Joshi, M. K., Jaiswar, M., Nanjappa, N., Purushottam, Yadav, R. K. S., Sharma, S., Pandey, S. B., Joshi, S., Joshi, Y. C., Lata, S., Mehdi, B. J., Misra, K. and Singh, M. (2018) 3.6-m Devasthal Optical Telescope Project: Completion and first results. *BSRSL*, 87, 29–41.
- Massaro, E., Maselli, A., Leto, C., Marchegiani, P., Perri, M., Giommi, P. and Piranomonte, S. (2015) The 5th edition of the Roma-BZCAT. A short presentation. *Ap&SS*, 357(1), 75. <https://doi.org/10.1007/s10509-015-2254-2>.
- Moore, R. L. and Stockman, H. S. (1984) A comparison of the properties of highly polarized QSOs versus low-polarization QSOs. *ApJ*, 279, 465–484. <https://doi.org/10.1086/161911>.

- Omar, A., Kumar, T., Reddy, B., Pant, J. and Mahto, M. (2019) First-light images from low-dispersion spectrograph-cum-imager on 3.6m devasthal optical telescope. *CSci*, 116, 1472–1478. <https://doi.org/10.18520/cs/v116/i9/1472-1478>.
- Peña-Herazo, H. A., Massaro, F., Gu, M., Paggi, A., Landoni, M., D’Abrusco, R., Ricci, F., Masetti, N. and Chavushyan, V. (2021) An Optical Overview of Blazars with LAMOST. I. Hunting Changing-look Blazars and New Redshift Estimates. *AJ*, 161(4), 196. <https://doi.org/10.3847/1538-3881/abe41d>.
- Punsly, B., Marziani, P., Zhang, S., Muzahid, S. and O’Dea, C. P. (2016) The Extreme Ultraviolet Variability of Quasars. *ApJ*, 830(2), 104. <https://doi.org/10.3847/0004-637X/830/2/104>.
- Rakshit, S., Stalin, C. S. and Kotilainen, J. (2020) Spectral Properties of Quasars from Sloan Digital Sky Survey Data Release 14: The Catalog. *ApJS*, 249(1), 17. <https://doi.org/10.3847/1538-4365/ab99c5>.
- Sagar, R. (1999) Some new initiatives in optical astronomy at UPSO, Nainital. *CSci*, 77, 643–652.
- Sagar, R., Stalin, C. S., Gopal-Krishna and Wiita, P. J. (2004) Intranight optical variability of blazars. *MNRAS*, 348, 176–186. <https://doi.org/10.1111/j.1365-2966.2004.07339.x>.
- Stalin, C. S., Gopal-Krishna, Sagar, R. and Wiita, P. J. (2004) Intranight optical variability of radio-quiet and radio lobe-dominated quasars. *MNRAS*, 350, 175–188. <https://doi.org/10.1111/j.1365-2966.2004.07631.x>.
- Stetson, P. B. (1987) DAOPHOT - A computer program for crowded-field stellar photometry. *PASP*, 99, 191–222. <https://doi.org/10.1086/131977>.
- Stetson, P. B. (1992) More Experiments with DAOPHOT II and WF/PC Images. In *Astronomical Data Analysis Software and Systems I*, edited by Worrall, D. M., Biemesderfer, C. and Barnes, J., vol. 25 of *Astronomical Society of the Pacific Conference Series*, p. 297.
- Stockman, H. S., Moore, R. L. and Angel, J. R. P. (1984) The optical polarization properties of “normal” quasars. *ApJ*, 279, 485–498. <https://doi.org/10.1086/161912>.
- Uchiyama, Y., Urry, C. M., Cheung, C. C., Jester, S., Van Duyne, J., Coppi, P., Sambruna, R. M., Takahashi, T., Tavecchio, F. and Maraschi, L. (2006) Shedding New Light on the 3C 273 Jet with the Spitzer Space Telescope. *ApJ*, 648(2), 910–921. <https://doi.org/10.1086/505964>.
- Uchiyama, Y., Urry, C. M., Coppi, P., Van Duyne, J., Cheung, C. C., Sambruna, R. M., Takahashi, T., Tavecchio, F. and Maraschi, L. (2007) An Infrared Study of the Large-Scale Jet in Quasar PKS 1136-135. *ApJ*, 661(2), 719–727. <https://doi.org/10.1086/518089>.
- Urry, C. M. and Padovani, P. (1995) Unified Schemes for Radio-Loud Active Galactic Nuclei. *PASP*, 107, 803. <https://doi.org/10.1086/133630>.

- Wagner, S. J. and Witzel, A. (1995) Intraday Variability In Quasars and BL Lac Objects. *ARA&A*, 33, 163–198. <https://doi.org/10.1146/annurev.aa.33.090195.001115>.
- Wills, B. J., Wills, D., Breger, M., Antonucci, R. R. J. and Barvainis, R. (1992) A Survey for High Optical Polarization in Quasars with Core-dominant Radio Structure: Is There a Beamed Optical Continuum? *ApJ*, 398, 454. <https://doi.org/10.1086/171869>.
- Xin, C., Charisi, M., Haiman, Z. and Schiminovich, D. (2020) Correlation between optical and UV variability of a large sample of quasars. *MNRAS*, 495(1), 1403–1413. <https://doi.org/10.1093/mnras/staa1258>.